



# Protein Tyrosine Phosphatase SHP2 Suppresses Host Innate Immunity against Influenza A Virus by Regulating EGFR-Mediated Signaling

Qingsen Wang,<sup>a</sup> Wenliang Pan,<sup>a</sup> Song Wang,<sup>a</sup> Chen Pan,<sup>a</sup> Hongya Ning,<sup>a</sup> Shile Huang,<sup>b,c</sup>  Shih-Hsin Chiu,<sup>a</sup> Ji-Long Chen<sup>a,d</sup>

<sup>a</sup>Key Laboratory of Fujian-Taiwan Animal Pathogen Biology, College of Animal Sciences (College of Bee Science), Fujian Agriculture and Forestry University, Fuzhou, China

<sup>b</sup>Department of Biochemistry and Molecular Biology, Louisiana State University Health Sciences Center, Shreveport, Louisiana, USA

<sup>c</sup>Feist-Weiller Cancer Center, Louisiana State University Health Sciences Center, Shreveport, Louisiana, USA

<sup>d</sup>CAS Key Laboratory of Pathogenic Microbiology and Immunology, Institute of Microbiology, Chinese Academy of Sciences, Beijing, China

Qingsen Wang and Wenliang Pan contributed equally to this work. Author order was determined in order of seniority. Also, Shih-Hsin Chiu and Ji-Long Chen contributed equally to this work.

**ABSTRACT** Influenza A virus (IAV) is a highly contagious pathogen, causing acute respiratory illnesses in human beings and animals and frequently giving rise to epidemic outbreaks. Evasion by IAV of host immunity facilitates viral replication and spread, which can be initiated through various mechanisms, including epidermal growth factor receptor (EGFR) activation. However, how EGFR mediates the suppression of antiviral systems remains unclear. Here, we examined host innate immune responses and their relevant signaling to EGFR upon IAV infection. IAV was found to induce the phosphorylation of EGFR and extracellular signal-regulated kinase (ERK) at an early stage of infection. Inhibition of EGFR or ERK suppressed the viral replication but increased the expression of type I and type III interferons (IFNs) and interferon-stimulated genes (ISGs), supporting the idea that IAV escapes from antiviral innate immunity by activating EGFR/ERK signaling. Meanwhile, IAV infection also induced the activation of Src homology region 2-containing protein tyrosine phosphatase 2 (SHP2). Pharmacological inhibition or small interfering RNA (siRNA)-based silencing of SHP2 enhanced the IFN-dependent antiviral activity and reduced virion production. Furthermore, knockdown of SHP2 attenuated the EGFR-mediated ERK phosphorylation triggered by viral infection or EGF stimulation. Conversely, ectopic expression of constitutively active SHP2 noticeably promoted ERK activation and viral replication, concomitant with diminished immune function. Altogether, the results indicate that SHP2 is crucial for IAV-induced activation of the EGFR/ERK pathway to suppress host antiviral responses.

**IMPORTANCE** Viral immune evasion is the most important strategy whereby viruses evolve for their survival. This work shows that influenza A virus (IAV) suppressed the antiviral innate immunity through downregulation of IFNs and ISGs by activating EGFR/ERK signaling. Meanwhile, IAV also induced the activation of protein tyrosine phosphatase SHP2, which was found to be responsible for modulating the EGFR-mediated ERK activity and subsequent antiviral effectiveness both *in vitro* and *in vivo*. The results suggest that SHP2 is a key signal transducer between EGFR and ERK and plays a crucial role in suppressing host innate immunity during IAV infection. The finding enhances our understanding of influenza immune evasion and provides a new therapeutic approach to viral infection.

**KEYWORDS** influenza A virus, innate immunity, interferon, EGFR, SHP2

**Citation** Wang Q, Pan W, Wang S, Pan C, Ning H, Huang S, Chiu S-H, Chen J-L. 2021. Protein tyrosine phosphatase SHP2 suppresses host innate immunity against influenza A virus by regulating EGFR-mediated signaling. *J Virol* 95:e02001-20. <https://doi.org/10.1128/JVI.02001-20>.

**Editor** Bryan R. G. Williams, Hudson Institute of Medical Research

**Copyright** © 2021 American Society for Microbiology. All Rights Reserved.

Address correspondence to Shih-Hsin Chiu, [shchiu@fafu.edu.cn](mailto:shchiu@fafu.edu.cn), or Ji-Long Chen, [chenjl@im.ac.cn](mailto:chenjl@im.ac.cn).

**Received** 9 October 2020

**Accepted** 13 December 2020

**Accepted manuscript posted online** 23 December 2020

**Published** 24 February 2021

Influenza A virus (IAV), a member of the family *Orthomyxoviridae*, is an enveloped virus whose genome contains eight segments of negative-sense single-stranded RNA, and it can cause severe respiratory diseases and seasonal epidemics worldwide (1, 2). IAV infection motivates host innate immune responses, including expression of type I and type III interferons (IFNs), through manifold transduction such as pathogen recognition receptor-mediated signaling (3–6). Consequently, IFNs trigger the activation of Janus kinase/signal transducer and activator of transcription (JAK/STAT), which upregulates the expression of interferon-stimulated genes (ISGs), thereby carrying out antiviral activities (7, 8). Nonetheless, IAV has evolved diverse strategies to evade the host antiviral system by variable genetic mutations or by employing cellular signaling, such as activation of epidermal growth factor receptor (EGFR).

EGFR is a transmembrane glycoprotein and member of the ErbB family of receptor tyrosine kinases, which consists of EGFR (ErbB1/HER1), ErbB2 (HER2/neu), ErbB3 (HER3), and ErbB4 (HER4). Activation of EGFR via dimerization and phosphorylation in tyrosine residues of its kinase domain stimulates multiple signaling pathways, which regulate a broad range of biological processes, including tissue homeostasis, as well as tumor progression and metastasis (9–11). Recently, it was reported that EGFR activation can be induced in response to various viruses, including IAV, and is involved in host immune defenses. In the case of IAV, binding of the virus to host cells induces the aggregation of plasma membrane lipids, which functions as a platform for activation of the EGFR signaling, which in turn facilitates virus internalization (12). The IAV-activated EGFR can cause a decrease in IFN- $\lambda$  and CXCL10 levels by downregulating the transcription factor IRF-1 (13, 14). The secretion of transforming growth factor  $\alpha$  (TGF- $\alpha$ ) stimulated by IAV infection also prompts the activation of EGFR and consequently promotes the expression of interleukin 8 (IL-8) and granulocyte-macrophage colony-stimulating factor (GM-CSF) cytokines (15). Moreover, the elevated production of the epithelial cell-derived mucin MUC5AC, which provides a protective barrier against pathogenic challenges, is triggered by transduction of a protease/EGFR/mitogen-activated protein kinase/extracellular signal-regulated kinase (MAPK/ERK)/specificity protein 1 (Sp1) cascade during IAV infection (16). On the other hand, the signaling of EGFR can be negatively regulated by SOCS5, resulting in viral restriction (17). Recently, purpurquinone B and fucoidan KW, derived from the acid-tolerant fungus *Penicillium purpurogenum* and the brown alga *Kjellmaniella crassifolia*, respectively, have been found to inhibit viral replication by interfering with activation of downstream molecules within the EGFR pathway (18, 19). Mounting evidence has suggested that EGFR-mediated signaling is a vital part of IAV infection, but how EGFR regulates the host innate immunity in response to IAV is still obscure.

Src homology region 2 (SH2)-containing protein tyrosine phosphatase 2 (SHP2), encoded by *PTPN11*, is a cytoplasmic nonreceptor protein tyrosine phosphatase which comprises two SH2 domains in the N-terminal half of SHP2 and one protein tyrosine phosphatase (PTP) domain in its C terminus (20–22). A conformational change evoked in the presence of extracellular stimulation of growth factors and cytokines, such as platelet-derived growth factor, epidermal growth factor (EGF), hepatocyte growth factor, ILs, and IFNs, prevents the SH2 domain from exerting inhibitory activity at the catalytic site in the PTP domain, which is concurrent with activation of its enzymatic property (23–30). In turn, SHP2 activation can regulate the activities of growth factor and cytokine receptors and their downstream signaling, which is intimately associated with development of normal tissues and various diseases, such as cancer (31–39). However, few studies have exploited the correlation between SHP2 and viral infection, especially IAV, so far.

Here, we examined the change in the expression pattern of EGFR-mediated signaling and IFNs in response to IAV infection and the outcomes. The results showed that IAV infection provoked the activation of SHP2 and ERK downstream of EGFR, and pharmacological or small interfering RNA (siRNA)-based inhibition of SHP2 suppressed virus production and enhanced innate immunity in alveolar epithelial cells and mice.

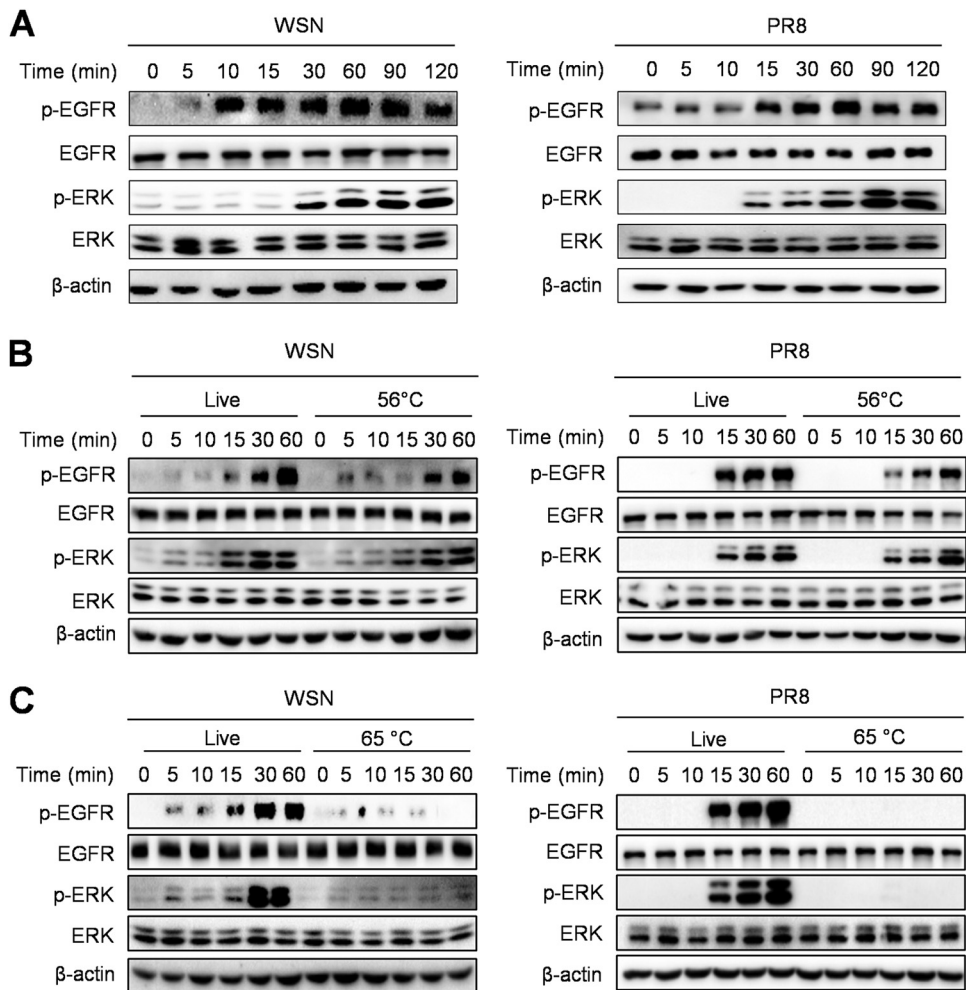


**FIG 1** IAV infection induces activation of the EGFR/ERK pathway. (A) A549 cells were infected with WSN or PR8 (MOI=1) and collected at 0, 5, 10, 15, 30, 60, 90, and 120 min. (B and C) A549 cells were infected with WSN or PR8 (MOI=1) without (Live) or with treatment at 56°C or 65°C, and then the cells were further cultured for 0, 5, 10, 15, 30, and 60 min. The cell lysates were harvested and subjected to Western blotting with the indicated antibodies.

Our findings indicate that SHP2 is activated during IAV infection and is able to modulate the EGFR/ERK signaling, leading to sustained viral replication via suppression of IFN-mediated antiviral immunity.

## RESULTS

**IAV activates the EGFR/ERK pathway at the early stage of infection.** To investigate whether the EGFR-mediated signaling is triggered by IAV infection, we examined the phosphorylation levels of EGFR and its downstream molecule ERK in cells infected with IAV, influenza virus A/WSN/33 (H1N1) (WSN), and influenza virus A/Puerto Rico/8/1934 (H1N1) (PR8). The immunoblotting results showed that IAV infection induced phosphorylation of EGFR and ERK within 30 min, and their activation was sustained for at least 2 h (Fig. 1A), indicating that the activation of the EGFR/ERK pathway occurs in host cells at the early time during IAV infection. It has been described that heat treatment at 56°C for 30 min allows IAV entry into cells but prevents viral replication, while increasing the temperature to 65°C is sufficient to completely inactivate viruses (40, 41). To determine whether the activation of the EGFR-mediated signaling is associated with virus invasion or viral replication, IAVs were treated at 56°C or at 65°C for 30 min.

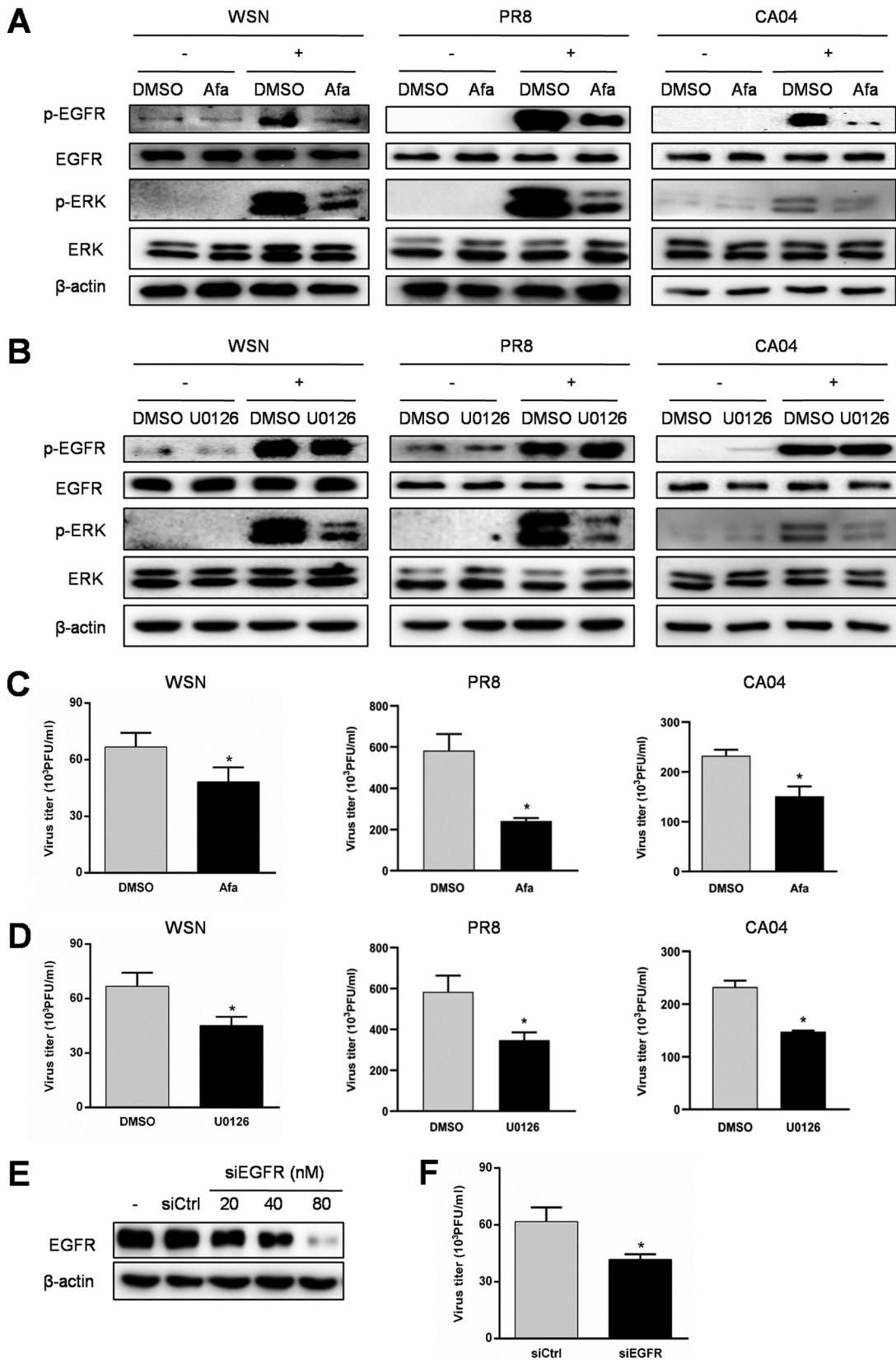


**FIG 2** Inhibition of the EGFR/ERK pathway reduces IAV replication. (A and B) A549 cells were pretreated with 1  $\mu$ M afatinib (Afa), 10  $\mu$ M U0126, or DMSO as a vehicle control for 12 h, followed by WSN, PR8, or CA04 infection (MOI = 1) for 30 min, and the protein samples were harvested. The expression levels of p-EGFR and p-ERK were detected by Western blotting. (C and D)

(Continued on next page)

We observed that the 56°C-treated viruses were able to induce the expression of p-EGFR and p-ERK, similar to the live control (Fig. 1B), whereas the 65°C-inactivated viruses failed to activate either of them (Fig. 1C). These results demonstrate that the EGFR/ERK pathway can be activated by IAV infection at the early invasion stage.

**The EGFR/ERK pathway is involved in IAV replication.** EGFR signaling participates in the replication of various viruses (13, 14, 42–46). However, the biological significance of the EGFR/ERK pathway in IAV replication remains to be elucidated. To determine whether the EGFR/ERK pathway plays an important role in IAV replication, cells were treated with afatinib and U0126, which can inhibit the activation of EGFR and ERK, respectively, prior to infection with WSN, PR8, or influenza virus A/California/04/2009 (H1N1) (CA04). As shown in Fig. 2A and B, afatinib extensively inhibited both p-EGFR and p-ERK, while U0126 blocked only p-ERK, in response to IAV infection. Inhibition of EGFR or ERK showed a significant decrease in virus titers in WSN, PR8, and CA04 infections (Fig. 2C and D). To confirm the role of EGFR in IAV replication, cells were transfected with EGFR siRNA (siEGFR). Treatment of siEGFR downregulated the EGFR protein level in a concentration-dependent manner (Fig. 2E) and also suppressed the virus production in comparison with the control (Fig. 2F). The above data support the idea that EGFR activation is responsible for IAV replication through its downstream ERK signaling.

**Inhibition of the EGFR/ERK pathway promotes antiviral innate immune response to IAV infection.** To understand how the EGFR/ERK pathway controls IAV infection, we evaluated the effect of this signaling on host antiviral innate immunity with regard to IFN responses. Inhibition of EGFR and ERK upregulated the mRNA levels of type I IFNs (IFN- $\alpha$  and IFN- $\beta$ ), type III IFNs (IL-29 and IL-28), and ISGs (ISG15 and MxA) during infection with WSN, PR8, and CA04 (Fig. 3A to F). Consistent with the change in the IFN mRNA expression, an increase in production of IFN- $\beta$  and IL-29 was observed in the culture supernatants (Fig. 3G and H). Furthermore, knockdown of EGFR also led to increases in the innate immunity-related gene expression (Fig. 4A and B) and IFN- $\beta$  and IL-29 secretion (Fig. 4C). Taken together, these results verify that activation of the EGFR/ERK pathway promotes IAV replication by suppressing the host innate immune response.

**SHP2 is required for IAV replication.** To explore the role of SHP2 in the regulation of IAV replication, we examined the activation status of SHP2 and its biological functions during IAV infection. The phosphorylation of SHP2 was induced within 30 min upon infection with WSN, PR8, and CA04 (Fig. 5A) and was suppressed by treatment with SHP099, an allosteric small molecule inhibitor of SHP2 (47), and siSHP2 in a concentration-dependent manner (Fig. 5B and C). Following inhibition or knockdown of SHP2, the production of infectious virions of WSN, PR8, and CA04 decreased significantly (Fig. 5D to G). Furthermore, administration of SHP099 effectively reduced IAV-induced phosphorylation of SHP2 and the expression of viral nucleoprotein (NP), as well as the titer of virus, in mice (Fig. 5H to J). Therefore, these results suggest that SHP2 is activated in response to IAV infection and is required for viral replication.

**Suppression of SHP2 enhances innate immunity against IAV.** To further determine the effect of SHP2 on host antiviral responses, we examined the expression pattern of innate immunity-related genes, including type I and type III IFNs and ISGs, during IAV infection after inhibition of SHP2. SHP099 treatment significantly increased the mRNA levels of IFNs and ISGs (Fig. 6A to D), as well as the secretion of IFN- $\beta$  and IL-29 (Fig. 6E), compared to vehicle controls. In line with this, siSHP2 treatment also elevated the expression levels of IFNs and ISGs, compared to the control siRNA treatment (Fig. 6F to H). These findings suggest that suppression of SHP2 may restore the host antiviral activity against IAV, leading to reduced viral replication.

## FIG 2 Legend (Continued)

Culture supernatants were harvested at 15 h postinfection and subjected to plaque assay to determine the virus titer. (E) A549 cells were transfected with siRNA corresponding to EGFR (siEGFR) or scrambled control siRNA (siCtrl) for 24 h, and the knockdown efficiency of siEGFR was determined by Western blotting. (F) After transfection with siEGFR or siCtrl at 80 nM for 24 h, the cells were exposed to WSN (MOI=1) for 15 h, and then the culture supernatants were collected for plaque assay. Data are means and standard deviations (SD). \*,  $P < 0.05$ .

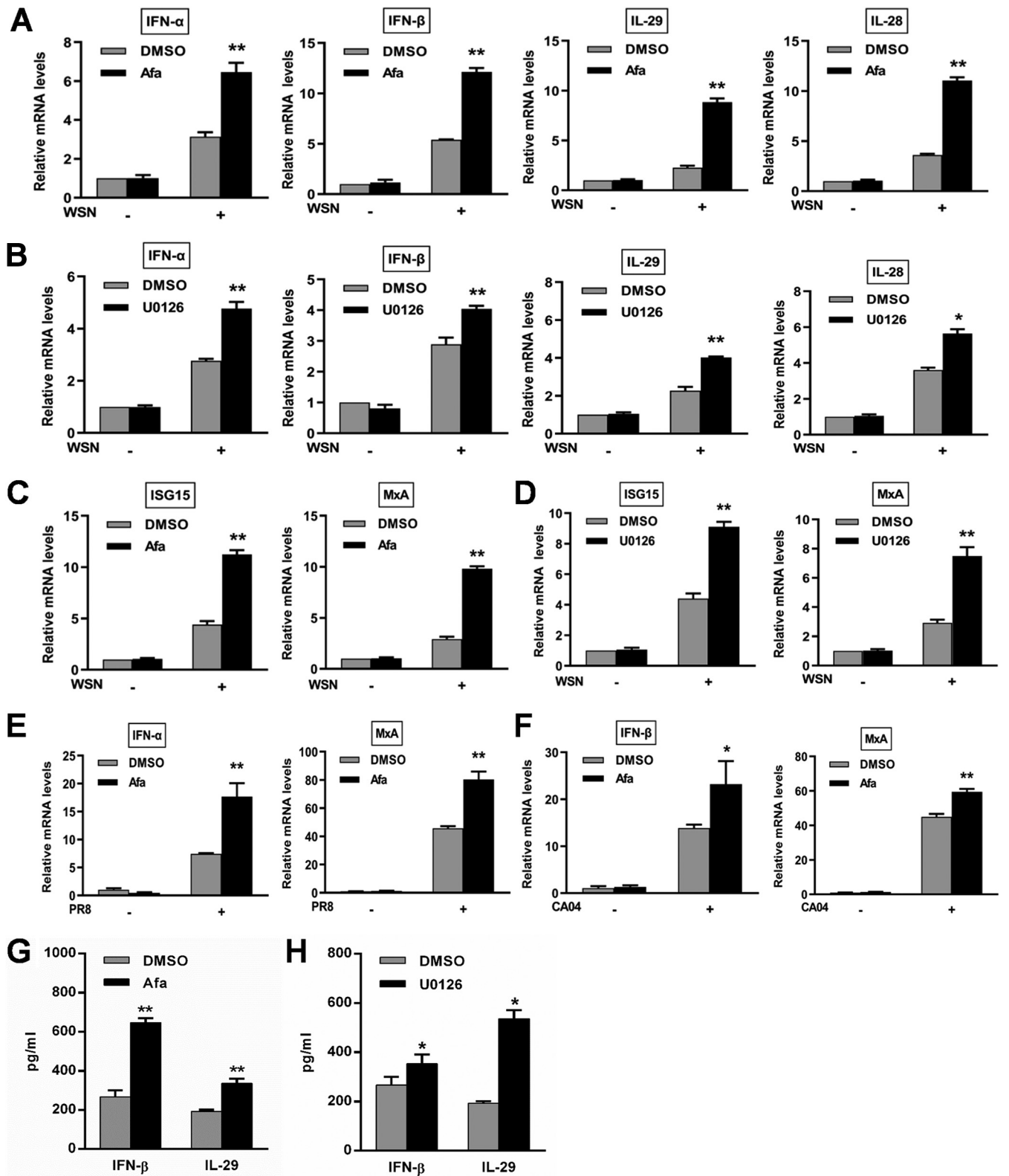


**FIG 3** Inhibition of IAV-induced EGFR/ERK signaling upregulates the expression of innate immunity-related genes. A549 cells were pretreated with 1  $\mu$ M afatinib (Afa) for 12 h, followed by infection with WSN (A and C), PR8 (E), or CA04 (F) (MOI=1). (B and D) After U0126 treatment at a concentration of 10  $\mu$ M for 12 h, A549 cells were infected with WSN (MOI=1). Total RNA was extracted at 8 h postinfection, and the mRNA levels of IFNs and ISGs were determined by qRT-PCR. (G and H) A549 cells were treated with 1  $\mu$ M Afa or 10  $\mu$ M U0126 prior to WSN infection (MOI=1). IFN- $\beta$  and IL-29 levels in the culture supernatants collected at 15 h postinfection were measured by ELISA. Data are means and SD. \*,  $P < 0.05$ ; \*\*,  $P < 0.01$ .

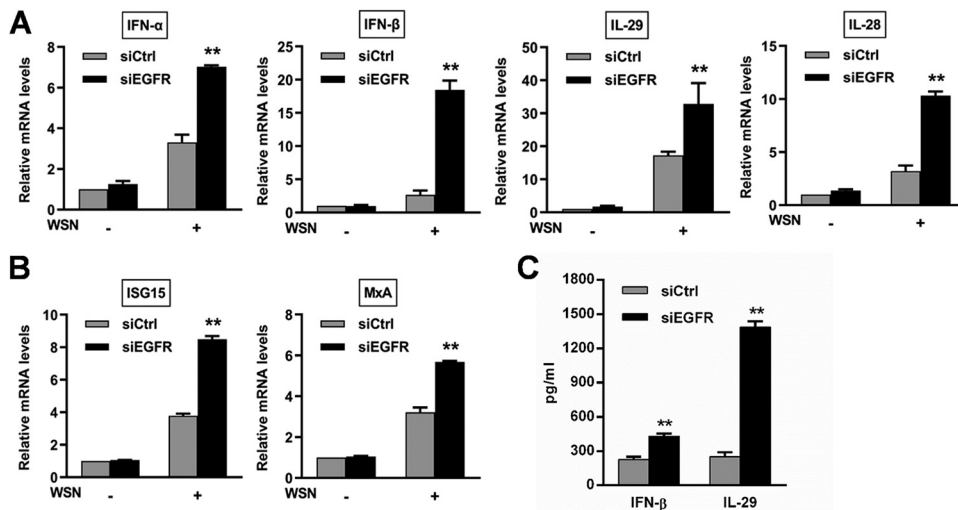


**FIG 4** Knockdown of EGFR upregulates the expression of innate immunity-related genes during IAV infection. A549 cells were transfected with siEGFR or scrambled control siRNA (siCtrl) at 80 nM for 24 h, followed by infection with WSN (MOI = 1). At 8 h postinfection, total RNA was extracted, and the mRNA levels of IFNs (A) and ISGs (B) were determined by qRT-PCR. (C) IFN- $\beta$  and IL-29 levels in the culture supernatants collected at 15 h postinfection were measured by ELISA. Data are means and SD. \*\*,  $P < 0.01$ .

**SHP2 regulates the EGFR/ERK pathway during IAV infection.** As observed from the results reported above, the EGFR/ERK signaling and SHP2 can be activated upon IAV infection, which reduces the host antiviral activity, thereby facilitating viral replication. Here, to investigate the interplay of the EGFR-mediated signaling and SHP2, siSHP2 and inhibitors specific to EGFR, SHP2, and ERK were used during IAV infection or EGF stimulation. As shown in Fig. 7A, EGF, a canonical EGFR ligand, triggered an increase in EGFR, ERK, and SHP2 phosphorylation, indicating that the SHP2 activation is associated with EGFR. Furthermore, knockdown of SHP2 robustly diminished WSN- and EGF-induced p-ERK without altering p-EGFR (Fig. 7B and C), suggesting that SHP2 functions as an intermediate between EGFR and ERK. In accordance with this observation, after viral infection or growth factor stimulation, lower levels of EGFR, SHP2, and ERK phosphorylation were manifested in the presence of afatinib compared to vehicle controls (Fig. 7D and E). SHP099 treatment markedly suppressed both p-SHP2 and p-ERK, while U0126 treatment inhibited only p-ERK (Fig. 7D and E). All of these demonstrate that SHP2 is a pivotal signal transducer between EGFR and ERK, in response to IAV infection.

**Activated SHP2 is required for activation of ERK and promotes viral replication.**

To confirm that SHP2 is an indispensable part of EGFR-mediated ERK activation during IAV infection, we generated wild-type SHP2 and a constitutively active mutant, SHP2 E76K (48, 49), and validated their biological activities by transfection of these constructs into host cells. The cells harboring SHP2 with the E76K active mutation exhibited an elevated phosphorylation level of downstream target ERK in comparison with empty vector and wild-type SHP2 groups (Fig. 8A). Following infection with WSN or PR8, ectopic expression of the SHP2 E76K intensified virus-induced phosphorylation of SHP2 and ERK and sufficiently counteracted the inhibitory potential of EGFR inhibitor afatinib on the ERK activation (Fig. 8B). Remarkably, the production of infectious virions was higher upon transfection of cells with the wild type and the constitutively active form of SHP2 than with the empty vector (Fig. 8C). In addition, IAV-induced expression of IFNs and ISGs was reduced after overexpression of wild-type SHP2 and SHP2 E76K (Fig. 8D). Therefore, these results suggest that SHP2 is capable of triggering ERK activation and promoting IAV replication.

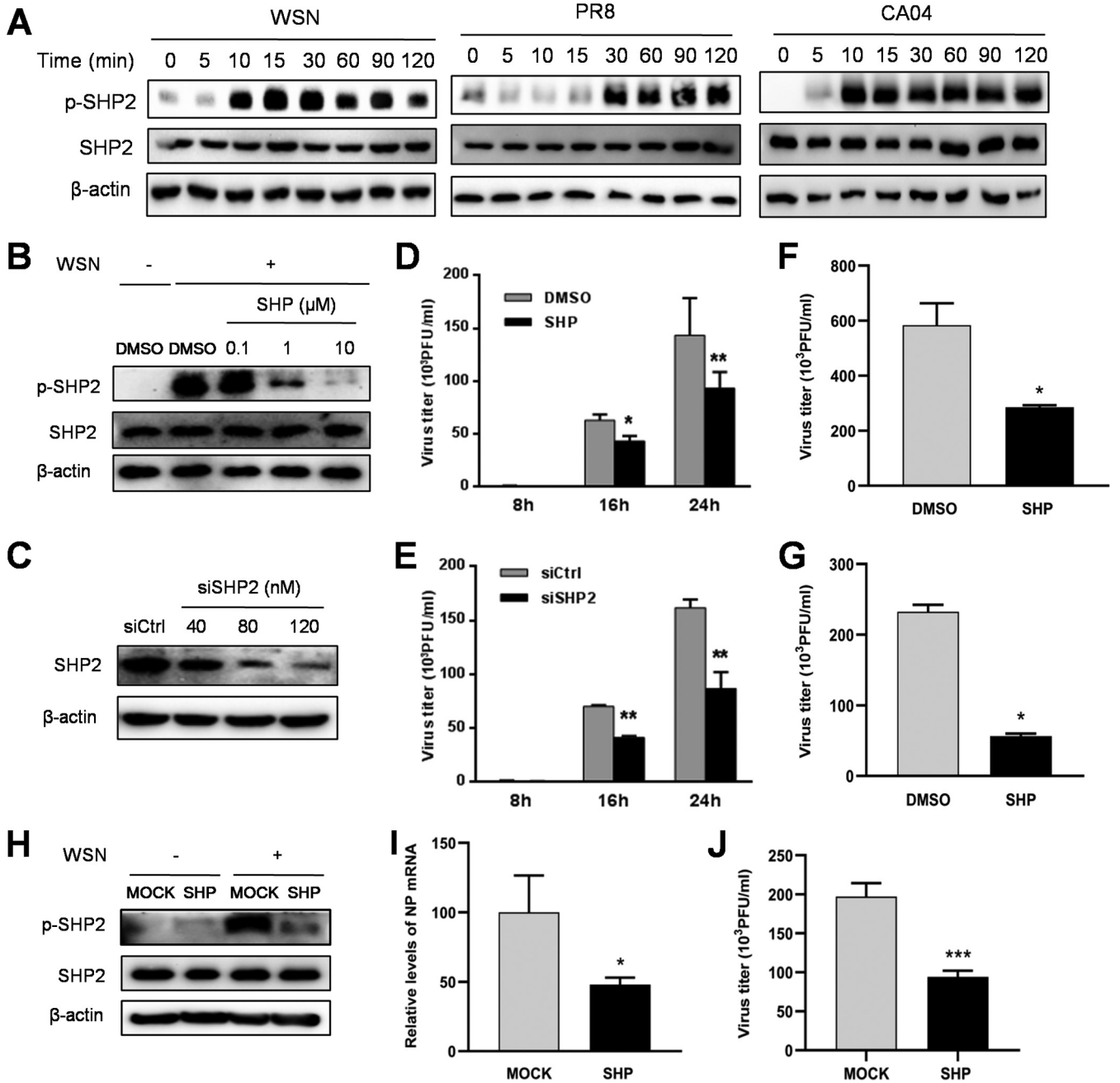


**FIG 5** Activation of SHP2 mediates IAV replication upon infection. (A) A549 cells were incubated with WSN, PR8, or CA04 (MOI=1) for 0, 5, 10, 15, 30, 60, 90, and 120 min prior to protein extraction and analysis using Western blotting with the indicated antibodies. (B and C) To examine the efficacy of SHP2 inhibitor and siRNA, A549 cells were treated with the SHP2 inhibitor SHP099 (SHP) for 12 h prior to infection with WSN (MOI=1) for 30 min or transfected with siRNA corresponding to SHP2 (siSHP2) or scrambled control siRNA (siCtrl) for 24 h. The cell lysates were analyzed by Western blotting with the indicated antibodies. The titer of WSN was determined by plaque assay at 8, 16, and 24 h postinfection (MOI=1) after pretreatment of cells with 10  $\mu$ M SHP099 for 12 h (D) or 120 nM siSHP2 for 24 h (E). A549 cells were pretreated with 10  $\mu$ M SHP099 for 12 h, followed by PR8 (F) or CA04 (G) infection (MOI=1) for 15 h, and then the culture supernatants were subjected to plaque assay to determine the virus titer. In mouse experiments, BALB/c mice were treated with SHP099 for 3 days prior to infection with WSN. At 24 h postinfection, lung homogenates of the mice ( $n=4$  per group; three independent experiments) were collected for assessing the phosphorylation status of SHP2 (H), the IAV NP mRNA level (I), and the virus titer (J). Data are means and SD. \*,  $P < 0.05$ ; \*\*,  $P < 0.01$ ; \*\*\*,  $P < 0.001$ .

**DISCUSSION**

In recent years, various strategies have been observed for viruses to achieve sustained viral replication, such as activating EGFR. To determine the role of EGFR in IAV replication, pharmacological and genetic approaches were utilized in this study. We found that inhibition of EGFR with its specific inhibitor (afatinib) or knockdown of



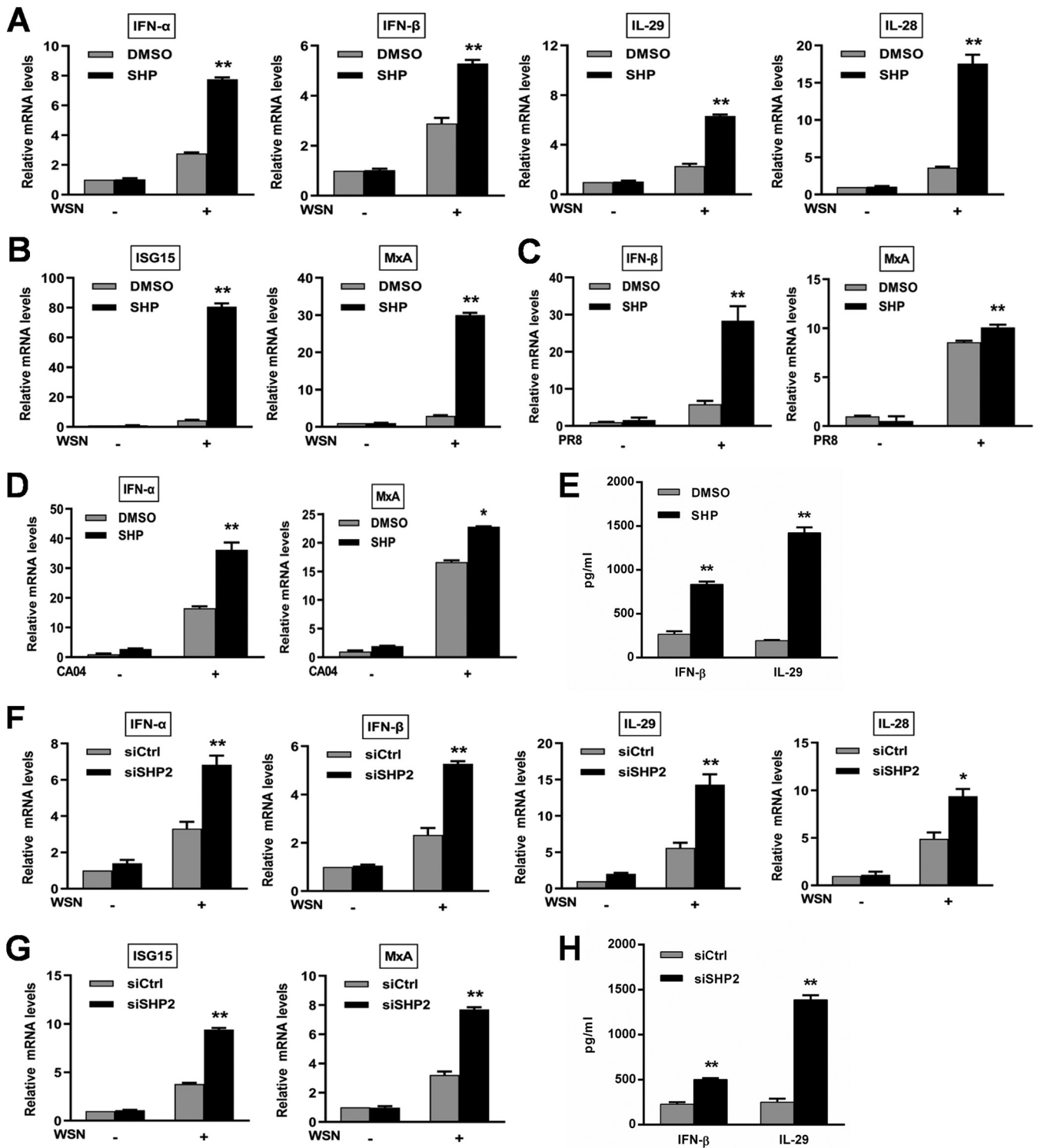


**FIG 6** Inhibition of IAV-induced SHP2 activation upregulates the expression of innate immunity-related genes. A549 cells were treated with 10  $\mu$ M SHP099 (SHP) for 12 h, followed by infection with WSN (A and B), PR8 (C), or CA04 (D) (MOI=1). A549 cells were transfected with siRNA corresponding to SHP2 (siSHP2) or scrambled control siRNA (siCtrl) at 120nM for 24 h prior to WSN infection (MOI=1) (F and G). After infection for 8 h, total RNA samples were harvested and subjected to qRT-PCR for assessing the levels of IFN and ISG mRNA. Following inhibition (E) and knockdown (H) of SHP2, IFN- $\beta$  and IL-29 levels in the culture supernatants collected at 15 h after WSN infection were measured by ELISA. Data are means and SD. \*,  $P < 0.05$ ; \*\*,  $P < 0.01$ .

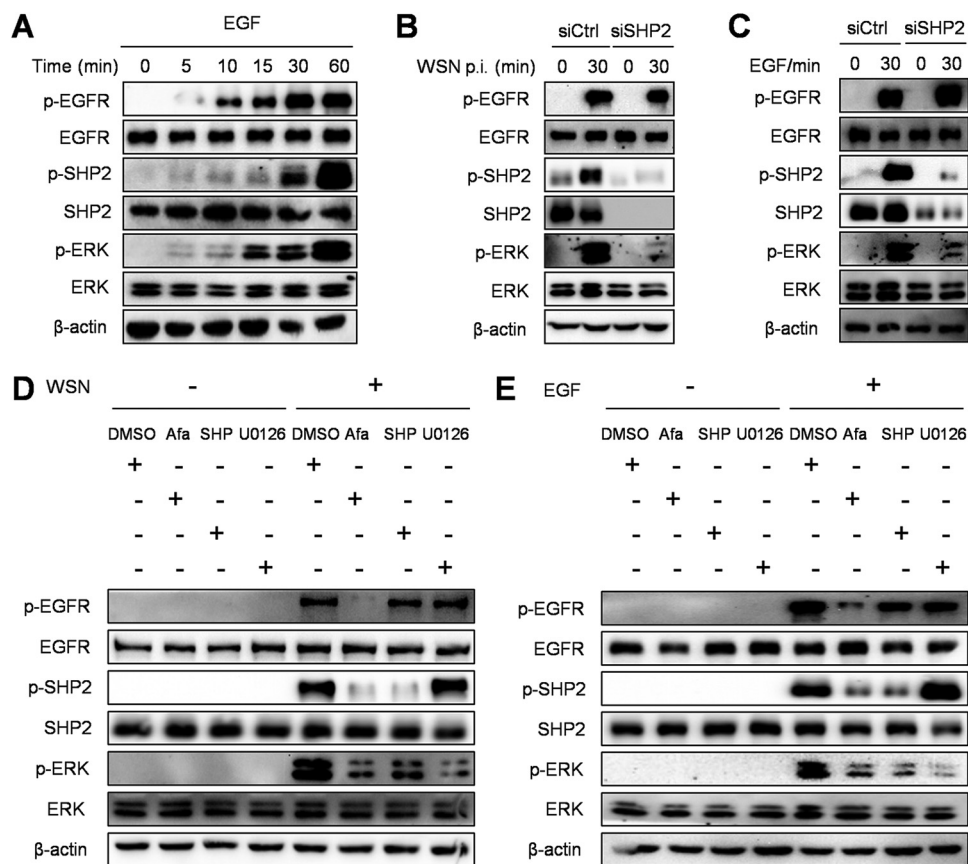


**FIG 7** SHP2 is involved in EGFR-mediated activation of ERK. (A) A549 cells were serum starved for 12 h and then treated with 10 ng/ml EGF for 0, 5, 10, 15, 30, and 60 min. The cell lysates were harvested and subjected to Western blotting with the indicated antibodies. (B and C) After transfection with siRNA corresponding to SHP2 (siSHP2) or scrambled control siRNA (siCtrl) at 120 nM for 24 h, A549 cells were infected with WSN (MOI = 1) or treated with 10 ng/ml EGF for 30 min, and the protein extracts were analyzed by Western blotting with the indicated antibodies. (D and E) A549 cells were pretreated with 1  $\mu$ M afatinib (Afa), 10  $\mu$ M SHP099 (SHP), or 10  $\mu$ M U0126 for 12 h and then infected with WSN (MOI = 1) or stimulated with 10 ng/ml EGF for 30 min. After incubation, the cell lysates were harvested and subjected to Western blotting with the indicated antibodies.

EGFR using siRNA enhanced the expression of type I and type III IFNs and ISGs and reduced the level of virion production during infection (Fig. 2 to 4), suggesting that IAV escapes from IFN-mediated antiviral immunity by activating the EGFR pathway. Our observation in IAV is in agreement with the previous findings in other viruses. For example, rhinovirus and respiratory syncytial virus infections induce the activation of EGFR, decreasing IRF-1-mediated IFN- $\lambda$  expression and increasing the virus production (13, 42). Porcine epidemic diarrhea virus infection or hepatitis C virus infection activates the EGFR/STAT3 signaling, downregulating the expression of type I IFN and ISGs (43, 44). Hepatitis B virus provokes the expression of EGFR and amphiregulin, a member of the EGF family, in intrahepatic regulatory T cells, which contributes to inhibiting CD8<sup>+</sup> T cell proliferation and antiviral activity (45); EGFR expression in hepatocytes is regulated by hepatitis B virus-encoded X gene product (HBx) (50, 51). The antiviral activity of the helicase DDX60, which carries out viral RNA degradation, is reduced along with EGFR activation in the presence of hepatitis C virus (46). In addition to host immunity, overexpression of EGFR commonly exists in nasopharyngeal and hepatocellular carcinomas harboring Epstein-Barr virus and hepatitis C virus, respectively (52, 53), and its hyperactivity elicited by severe acute respiratory syndrome coronavirus results in the progression to pulmonary fibrosis (54). Taking these findings into account, EGFR is strongly implicated in viral immune evasion and pathogenesis.

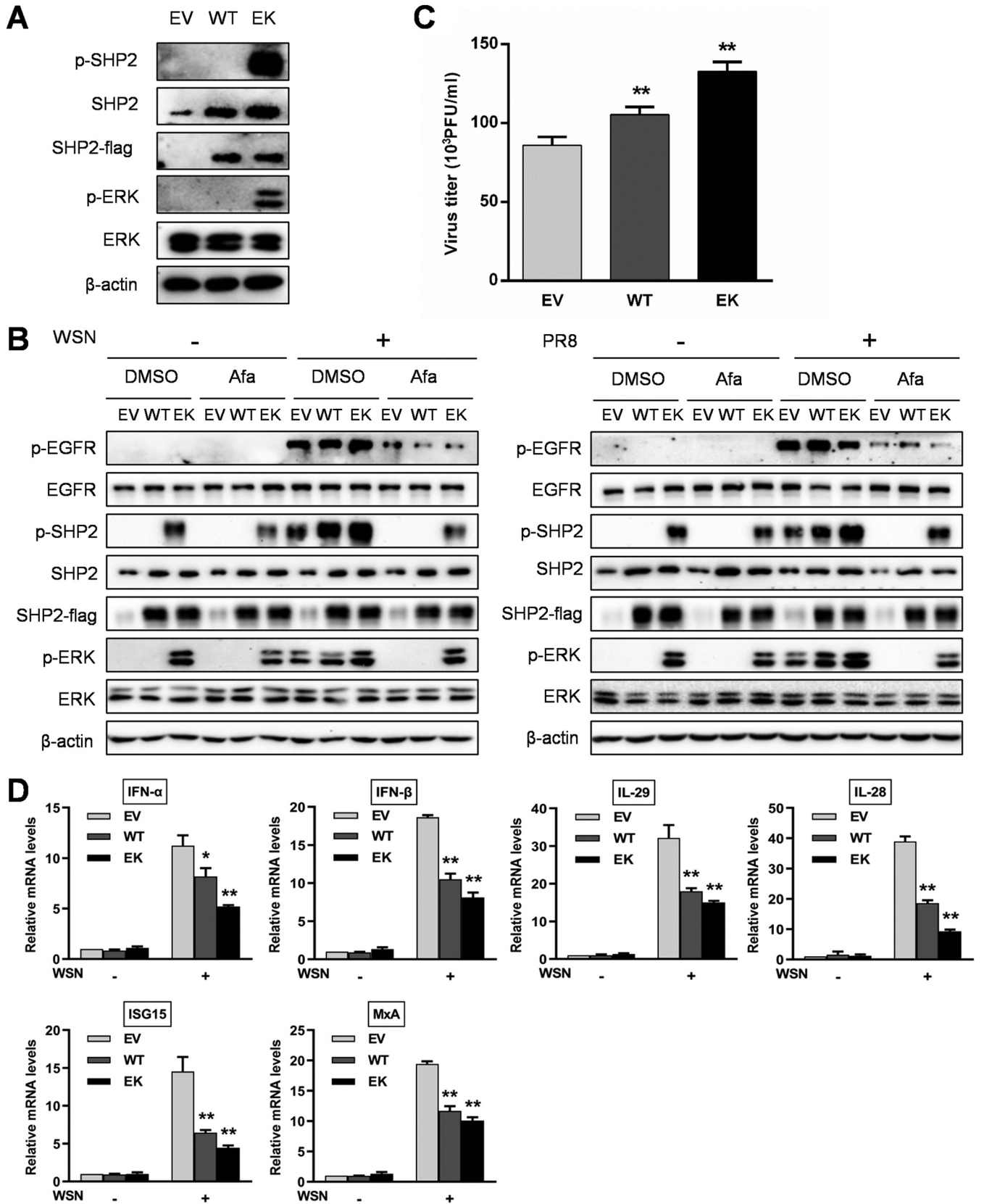


**FIG 8** Activated SHP2 is required for ERK activation and promotes IAV replication. (A) A549 cells were transiently transfected with empty vector (EV), wild-type SHP2 (WT), or a constitutively active SHP2 mutant (EK) for 24 h, followed by protein extraction and analysis using Western blotting with the indicated antibodies. (B) A549 cells harboring EV, WT, or EK were pretreated with or without 1 μM afatinib (Afa) for 12 h and then infected with WSN or PR8 (Continued on next page)

EGFR orchestrates a complex network through diverse intermediates, including MAPK/ERK, phosphoinositide 3-kinase (PI3K)/Akt, JAK/STAT, protein kinase C (PKC), and phospholipase C $\gamma$  (PLC $\gamma$ ), which is involved in multiple cell functions (55). To address which effector downstream of EGFR is required for IAV immune evasion, and host innate immunity in particular, U0126, a selective inhibitor that inhibits activation of MAPK, was employed. The results showed that U0126 treatment resulted in an obvious upregulation of the immune activity mediated by IFNs and subsequent suppression of viral replication (Fig. 2 and 3), whereas inhibition of PI3K/Akt or nuclear factor  $\kappa$ B (NF- $\kappa$ B) had no such effects (data not shown). Furthermore, IAV-induced phosphorylation of ERK was drastically attenuated by treatment with the EGFR inhibitor (Fig. 1, 2, 7, and 8). Thus, these results indicate that ERK signaling is the target of EGFR, being crucial for IAV escaping from the innate immunity. A previous study has shown that administration of purpurquinone B, an antiviral agent, is able to reduce the production of IAV virions and inflammatory factors, such as tumor necrosis factor alpha (TNF- $\alpha$ ), IL-6, RANTES, and keratinocyte-derived chemokine (KC), by blocking the ERK and NF- $\kappa$ B pathways (18). EGFR-induced activation of ERK also increases MUC5AC secretion for clearance of adherent IAV from the epithelium (16). In addition, IAV endocytosis is suppressed by inhibiting EGFR downstream molecules, PI3K/Akt and NF- $\kappa$ B, by fucoidan KW treatment (19). Collectively, IAV has the capacity to trigger multiple functional outcomes by initiating different signals downstream of EGFR.

The biological significance of SHP2 has been extensively studied in the field of tumorigenesis, but the role of SHP2 in the virus life cycle is poorly understood. Early research showed that costimulation with envelope proteins of hepatitis C virus and human immunodeficiency virus, E2 and gp120, respectively, in hepatocytes concertedly activates p38 and SHP2, which enhances liver injury by AP-1-mediated upregulation of IL-8 (56). SHP2, while being activated by infection with human cytomegalovirus, directly interacts with STAT1 and in turn inhibits the phosphorylation of STAT1 induced by IFN- $\gamma$  (57). Moreover, Kaposi's sarcoma-associated herpesvirus vGPCR initiates activation of ERK, NF- $\kappa$ B, and AP-1, which requires the participation of SHP2, for exacerbating tumor progression (58, 59). In peripheral blood CD4<sup>+</sup> T cells from simian immunodeficiency virus-infected rhesus macaques, the suppressed Th17 expression is associated with upregulation of several cellular regulators, including SHP2 (60). In the present study, we found that IAV infection induced the phosphorylation of SHP2, and inhibition of SHP2 reduced the production of infectious virions, which was likely attributable to the upregulated expression of IFNs and ISGs in cells (Fig. 5 and 6). Higher expression levels of innate immunity-related genes were also observed in mice upon administration of SHP2 inhibitor (data not shown). In contrast, ectopic expression of constitutively activated SHP2 increased the virus titer (Fig. 8). Of note, a recent study showed that mice with SHP2 deficiency have an enhanced susceptibility to postinfluenza *Staphylococcus aureus* infection due to overproduction of type I IFNs but show no apparent effect on influenza virus production (61). The infectious dose in the earlier work was 200 PFU, which is much lower than the dose we used for challenging mice (Fig. 5). Therefore, these observations imply that SHP2 activation upon IAV infection is able to attenuate the antiviral innate immunity.

SHP2 functions as a signal transducer between receptor tyrosine kinases and their downstream signaling molecules, such as MAPK/ERK, PI3K/Akt, and STAT, which modulates cell proliferation, apoptosis, differentiation, DNA damage and replication, and drug resistance (29, 62, 63). Here, we noticed that IAV infection triggered the phosphorylation of EGFR and the downregulation of IFNs and ISGs (Fig. 1, 3, and 4). To explore the possible mechanism by which EGFR mediates viral immune evasion, the MAPK/ERK

#### FIG 8 Legend (Continued)

(MOI=1) for 30 min. After infection, the cell lysates were harvested and subjected to Western blotting with the indicated antibodies. (C) A549 cells harboring EV, WT, or EK were infected with WSN (MOI=1). The culture supernatants were collected at 15 h postinfection, and the virus titer was determined by plaque assay. (D) A549 cells harboring EV, WT, or EK were infected with WSN (MOI=1) for 8 h. Total RNA was extracted after infection, and the mRNA levels of IFNs and ISGs were assessed by qRT-PCR. Data are means and SD. \*,  $P < 0.05$ ; \*\*,  $P < 0.01$ .

and PI3K/Akt pathways downstream of EGFR were examined. We found that inhibition of ERK (Fig. 3), but not PI3K (data not shown), enhanced the expression of IFNs and ISGs. Knockdown of SHP2 resulted in reduced phosphorylation of ERK in response to viral infection or EGF stimulation, whereas overexpression of SHP2 exhibited the opposite effect (Fig. 7 and 8), demonstrating that the MAPK/ERK signaling is a key target downstream of SHP2 and crucial for IAV infection. Furthermore, inhibition of EGFR abrogated the phosphorylation of both of SHP2 and ERK (Fig. 7 and 8). These results support the idea that SHP2 is a critical signal transducer between EGFR and ERK during IAV infection. In this study, we also noticed that inhibition or knockdown of SHP2 enhanced the expression of phosphorylated STAT1 during the early course of IAV infection (data not shown). However, the association between SHP2-induced STAT1 activation and innate immunity against IAV remains unclear and is worthy of further investigation. In comparison to HBx-mediated SHP2 expression via NF- $\kappa$ B transcription, which participates in the regulation of the EGFR/ERK signaling in liver fibrogenesis (64), we found here that IAV infection increased the phosphorylation level rather than the total protein level of SHP2 (Fig. 5). Taken together, our results indicate that IAV mediates the EGFR/ERK pathway for escaping host innate immunity through activation of SHP2.

## MATERIALS AND METHODS

**Viruses and cells.** Influenza viruses A/WSN/33 (H1N1) (WSN), A/Puerto Rico/8/1934 (H1N1) (PR8), and A/California/04/2009 (H1N1) (CA04) were propagated in specific-pathogen-free embryonated chicken eggs as previously described (65, 66). The virus titer was determined by plaque assay using Madin-Darby canine kidney (MDCK) cells (67). For viral infection, cells were infected with viruses at a multiplicity of infection (MOI) of 1 in Dulbecco's modified Eagle's medium (DMEM; HyClone) containing 2  $\mu$ g/ml TPCK (L-1-tosylamido-2-phenylethyl chloromethyl ketone)-treated trypsin, 100 U/ml penicillin, and 100  $\mu$ g/ml streptomycin for 1 h at 37°C. After adsorption, the supernatant was aspirated, and then the cells were washed with phosphate-buffered saline (PBS) to remove noninternalized viral particles and cultured in fresh DMEM containing 2  $\mu$ g/ml trypsin for subsequent analysis. Adenocarcinomic human alveolar basal epithelial cells, A549 cells, and MDCK cells obtained from the American Type Culture Collection (ATCC) were cultured in DMEM supplemented with 10% heat-inactivated fetal bovine serum (FBS; Gibco, Thermo Fisher Scientific), 2 mM glutamine, 100 U/ml penicillin, and 100  $\mu$ g/ml streptomycin at 37°C in a 5% CO<sub>2</sub> humidified atmosphere.

**Drug treatment.** For inhibition of protein activity, cells were treated with the EGFR inhibitor afatinib (Selleck), the SHP2 inhibitor SHP099 (Selleck), the ERK inhibitor U0126 (Selleck), or dimethyl sulfoxide (DMSO) as a vehicle control for 12 h, and then the cells were infected with IAV for 0.5, 8, 15, 16, or 24 h in the presence of inhibitors. For EGF stimulation, cells were serum starved for 12 h prior to addition of EGF (Novoprotein) for 0, 5, 10, 15, 30, and 60 min.

**RNA interference, plasmid construction, and transfection.** For gene knockdown, EGFR small interfering RNA (siRNA) (no. sc-29301), SHP2 siRNA (no. sc-36488), and their scrambled control siRNAs (no. sc-37007) were purchased from Santa Cruz Biotechnology. For ectopic expression, the total RNA acquired from cells with a total RNA kit (Omega Bio-tek) was reverse transcribed into cDNA using ReverTra Ace qPCR RT master mix (Toyobo), and the coding region of the SHP2 gene, according to the recently updated sequence available in NCBI GenBank (accession no. [NM\\_002834.5](#)), was amplified by PCR. The amplicon was cloned into the eukaryotic expression vector pFLAG-CMV-5a at the BamHI and EcoRI cloning sites. Lysine substitution of the glutamic acid residue at amino acid 76 of SHP2 generated a constitutively active gain-of-function mutant by site-directed mutagenesis using a fast mutagenesis kit (Vazyme). Cells were transfected with siRNAs or plasmids using Lipofectamine 2000 according to the manufacturer's instructions (Invitrogen). At 24 h posttransfection, the cells were infected with IAV or stimulated with EGF, followed by further analysis. The primer sequences are listed in Table 1.

**Western blotting.** Cell extracts were harvested in cell lysis buffer (Cell Signaling Technology) for 30 min on ice and then centrifuged at 12,000  $\times$  g for 15 min at 4°C to collect the supernatants. The lysates were mixed with a sample buffer (Solarbio), followed by heat treatment at 95°C for 5 min. The samples were separated by SDS-polyacrylamide gel electrophoresis (SDS-PAGE) and then transferred onto Immobilon-NC membranes (Merck) at 250 mA for 120 min in a cold room. The membrane was soaked in 5% skim milk at room temperature for 1 h. After blocking, the membrane was incubated with primary antibodies specific to EGFR, phospho-EGFR (Y1068), SHP2, phospho-SHP2 (Y542), ERK, phospho-ERK (T202/Y204) (Cell Signaling Technology),  $\beta$ -actin, and Flag (TransGen) at 4°C overnight prior to treatment with horseradish peroxidase-conjugated goat anti-mouse and -rabbit IgG at room temperature incubation for 1.5 h. The protein band was developed with NcmECL Ultra Reagent (NCM Biotech) and detected using a FluorChem M imaging system (ProteinSimple).

**Plaque assay.** MDCK cells were seeded in 12-well plates overnight and then incubated with serial dilutions of culture supernatants for 2 h. After incubation, the cells were washed and overlaid with DMEM containing 0.6% low-melting-point agarose and 2  $\mu$ g/ml TPCK-trypsin at 4°C for 30 min.

**TABLE 1** PCR primers used in this study

Primer <sup>a</sup>	Sequence (5'–3')
SHP2-EcoR1-F	AGCTCGTTTAGTGACCGTCAGAAATTCATGACATCGCGGAGATGG
SHP2-BamHI-R	TCGTCCTTGTAAATCGGTACCGGATCCTCTGAAACTTTTCTGCTGTTG
IFN- $\alpha$ -F	TGAATGACCTGGAAGCCTGT
IFN- $\alpha$ -R	TGATTTCTGCTCTGACAACCTC
IFN- $\beta$ -F	GCTACAACCTGCTTGGATTCC
IFN- $\beta$ -R	TGTCCTTGAGGCAGTATTCA
IL-29-F	TGCTGGTGACTTTGGTGCTA
IL-29-R	TGTGGTGACAGAGATTTGAACC
IL-28-F	CCACATAGCCAGTTCAA
IL-28-R	AAGCGACTTCTAAGGCA
GAPDH-F	CTGGGCTACACTGAGCAC
GAPDH-R	AAGTGGTCGTTGAGGGCAATG
IAV NP-F	TCAAACGTGGGATCAATG
IAV NP-R	GTGCAGACCGTCTAGAA

<sup>a</sup>F, forward; R, reverse.

Following this, the plates were placed upside down at 37°C for a further 72 h. Visible plaques were counted for virus titer determination.

**Ethics statement.** All animal experiments in this study were carried out in accordance with the Regulations for the Administration of Affairs Concerning Experimental Animals approved by the State Council of People's Republic of China. The animal protocol was reviewed and approved by the Research Ethics Committee of College of Animal Sciences (College of Bee Science), Fujian Agriculture and Forestry University (permit number PZCASFAFU2017003).

**Mouse experiment.** Female BALB/c mice (5 to 6 weeks old, 18 to 20 g) were purchased from Shanghai SLAC Laboratory Animal Co., Ltd. Mice were treated with the orally bioavailable SHP2 inhibitor SHP099 (75 mg/kg/day) via an intragastric route for 3 days, and then the mice were anaesthetized and inoculated intranasally with  $5 \times 10^4$  PFU of WSN. At 24 h postinfection, lung tissues were excised from the mice after euthanization and collected for further analysis.

**Quantitative reverse transcription-PCR.** Total RNA was isolated from cells using a total RNA kit (Omega Bio-tek) and then reverse transcribed into cDNA with a ReverTra Ace qPCR RT master mix (Toyobo). The cDNA samples were mixed with primers and SYBR green master Rox (TransGen). The qPCR was performed using a LightCycler 96 instrument (Roche) with the following cycling program: initial denaturation at 94°C for 30 s and 45 cycles of denaturation at 94°C for 5 s, annealing at 58°C for 15 s, and extension at 72°C for 10 s. The primer sequences are listed in Table 1.

**Cytokine release assay.** Culture supernatants were collected at 15 h after virus infection, and the levels of IFN- $\beta$  and IL-29 were measured with an IFN- $\beta$  enzyme-linked immunosorbent assay (ELISA) kit (Elabscience) and IL-29 ELISA kit (Cusabio), respectively, according to the manufacturer's protocols.

**Statistical analysis.** Statistical analysis was performed using Student's *t* test. A *P* value of less than 0.05 was considered statistically significant.

## ACKNOWLEDGMENTS

This work was supported by the National Key Research and Development Program of China (2016YFD0500205), the National Natural Science Foundation of China (U1805231 and 32030110), and the Natural Science Foundation of Fujian Province, China (2020J06016 and 2020J01539).

## REFERENCES

1. Taubenberger JK, Kash JC. 2010. Influenza virus evolution, host adaptation, and pandemic formation. *Cell Host Microbe* 7:440–451. <https://doi.org/10.1016/j.chom.2010.05.009>.
2. Long JS, Mistry B, Haslam SM, Barclay WS. 2019. Host and viral determinants of influenza A virus species specificity. *Nat Rev Microbiol* 17:67–81. <https://doi.org/10.1038/s41579-018-0115-z>.
3. Pichlmair A, Schulz O, Tan CP, Naslund TI, Liljestrom P, Weber F, Reis e Sousa C. 2006. RIG-I-mediated antiviral responses to single-stranded RNA bearing 5'-phosphates. *Science* 314:997–1001. <https://doi.org/10.1126/science.1132998>.
4. Lund JM, Alexopoulou L, Sato A, Karow M, Adams NC, Gale NW, Iwasaki A, Flavell RA. 2004. Recognition of single-stranded RNA viruses by Toll-like receptor 7. *Proc Natl Acad Sci U S A* 101:5598–5603. <https://doi.org/10.1073/pnas.0400937101>.
5. Schulz O, Diebold SS, Chen M, Naslund TI, Nolte MA, Alexopoulou L, Azuma YT, Flavell RA, Liljestrom P, Reis e Sousa C. 2005. Toll-like receptor 3 promotes cross-priming to virus-infected cells. *Nature* 433:887–892. <https://doi.org/10.1038/nature03326>.
6. Wei H, Wang S, Chen Q, Chen Y, Chi X, Zhang L, Huang S, Gao GF, Chen JL. 2014. Suppression of interferon lambda signaling by SOCS-1 results in their excessive production during influenza virus infection. *PLoS Pathog* 10:e1003845. <https://doi.org/10.1371/journal.ppat.1003845>.
7. Lenschow DJ, Lai C, Frias-Staheli N, Giannakopoulos NV, Lutz A, Wolff T, Osiak A, Levine B, Schmidt RE, Garcia-Sastre A, Leib DA, Pekosz A, Knobeloch KP, Horak I, Virgin HW. 2007. IFN-stimulated gene 15 functions as a critical antiviral molecule against influenza, herpes, and Sindbis viruses. *Proc Natl Acad Sci U S A* 104:1371–1376. <https://doi.org/10.1073/pnas.0607038104>.
8. Staeheli P, Haller O, Boll W, Lindenmann J, Weissmann C. 1986. Mx protein: constitutive expression in 3T3 cells transformed with cloned Mx

- cDNA confers selective resistance to influenza virus. *Cell* 44:147–158. [https://doi.org/10.1016/0092-8674\(86\)90493-9](https://doi.org/10.1016/0092-8674(86)90493-9).
9. Wong RW, Guillaud L. 2004. The role of epidermal growth factor and its receptors in mammalian CNS. *Cytokine Growth Factor Rev* 15:147–156. <https://doi.org/10.1016/j.cytogfr.2004.01.004>.
  10. Richani D, Gilchrist RB. 2018. The epidermal growth factor network: role in oocyte growth, maturation and developmental competence. *Hum Reprod Update* 24:1–14. <https://doi.org/10.1093/humupd/dmx029>.
  11. Guardiola S, Varese M, Sanchez-Navarro M, Giralte E. 2019. A third shot at EGFR: new opportunities in cancer therapy. *Trends Pharmacol Sci* 40:941–955. <https://doi.org/10.1016/j.tips.2019.10.004>.
  12. Eierhoff T, Hrinčius ER, Rescher U, Ludwig S, Ehrhardt C. 2010. The epidermal growth factor receptor (EGFR) promotes uptake of influenza A viruses (IAV) into host cells. *PLoS Pathog* 6:e1001099. <https://doi.org/10.1371/journal.ppat.1001099>.
  13. Ueki IF, Min-Oo G, Kalinowski A, Ballon-Landa E, Lanier LL, Nadel JA, Koff JL. 2013. Respiratory virus-induced EGFR activation suppresses IRF1-dependent interferon lambda and antiviral defense in airway epithelium. *J Exp Med* 210:1929–1936. <https://doi.org/10.1084/jem.20121401>.
  14. Kalinowski A, Ueki I, Min-Oo G, Ballon-Landa E, Knoff D, Galen B, Lanier LL, Nadel JA, Koff JL. 2014. EGFR activation suppresses respiratory virus-induced IRF1-dependent CXCL10 production. *Am J Physiol Lung Cell Mol Physiol* 307:L186–L196. <https://doi.org/10.1152/ajplung.00368.2013>.
  15. Ito Y, Correll K, Zemans RL, Leslie CC, Murphy RC, Mason RJ. 2015. Influenza induces IL-8 and GM-CSF secretion by human alveolar epithelial cells through HGF/c-Met and TGF-alpha/EGFR signaling. *Am J Physiol Lung Cell Mol Physiol* 308:L1178–L1188. <https://doi.org/10.1152/ajplung.00290.2014>.
  16. Barbier D, Garcia-Verdugo I, Pothlichet J, Khazen R, Descamps D, Rousseau K, Thornton D, Si-Tahar M, Touqui L, Chignard M, Sallenave JM. 2012. Influenza A induces the major secreted airway mucin MUC5AC in a protease-EGFR-extracellular regulated kinase-Sp1-dependent pathway. *Am J Respir Cell Mol Biol* 47:149–157. <https://doi.org/10.1165/rcmb.2011-0405OC>.
  17. Kedzierski L, Tate MD, Hsu AC, Kolesnik TB, Linossi EM, Dagley L, Dong Z, Freeman S, Infusini G, Starkey MR, Bird NL, Chatfield SM, Babon JJ, Huntington N, Belz G, Webb A, Wark PA, Nicola NA, Xu J, Kedzierska K, Hansbro PM, Nicholson SE. 2017. Suppressor of cytokine signaling (SOCS) 5 ameliorates influenza infection via inhibition of EGFR signaling. *Elife* 6:e20444. <https://doi.org/10.7554/eLife.20444>.
  18. Wang M, Wang S, Wang W, Wang Y, Wang H, Zhu W. 2017. Inhibition effects of novel polyketide compound PPQ-B against influenza A virus replication by interfering with the cellular EGFR pathway. *Antiviral Res* 143:74–84. <https://doi.org/10.1016/j.antiviral.2017.04.007>.
  19. Wang W, Wu J, Zhang X, Hao C, Zhao X, Jiao G, Shan X, Tai W, Yu G. 2017. Inhibition of influenza A virus infection by fucoidan targeting viral neuraminidase and cellular EGFR pathway. *Sci Rep* 7:40760. <https://doi.org/10.1038/srep40760>.
  20. Chan RJ, Feng GS. 2007. PTPN11 is the first identified proto-oncogene that encodes a tyrosine phosphatase. *Blood* 109:862–867. <https://doi.org/10.1182/blood-2006-07-028829>.
  21. Barford D, Neel BG. 1998. Revealing mechanisms for SH2 domain mediated regulation of the protein tyrosine phosphatase SHP-2. *Structure* 6:249–254. [https://doi.org/10.1016/s0969-2126\(98\)00027-6](https://doi.org/10.1016/s0969-2126(98)00027-6).
  22. Neel BG. 1993. Structure and function of SH2-domain containing tyrosine phosphatases. *Semin Cell Biol* 4:419–432. <https://doi.org/10.1006/scel.1993.1050>.
  23. Feng GS, Hui CC, Pawson T. 1993. SH2-containing phosphotyrosine phosphatase as a target of protein-tyrosine kinases. *Science* 259:1607–1611. <https://doi.org/10.1126/science.8096088>.
  24. Feng GS, Shen R, Heng HH, Tsui LC, Kazlaszkas A, Pawson T. 1994. Receptor-binding, tyrosine phosphorylation and chromosome localization of the mouse SH2-containing phosphotyrosine phosphatase Syp. *Oncogene* 9:1545–1550.
  25. Fuhrer DK, Feng GS, Yang YC. 1995. Syp associates with gp130 and Janus kinase 2 in response to interleukin-11 in 3T3-L1 mouse preadipocytes. *J Biol Chem* 270:24826–24830. <https://doi.org/10.1074/jbc.270.42.24826>.
  26. Bennett AM, Tang TL, Sugimoto S, Walsh CT, Neel BG. 1994. Protein-tyrosine-phosphatase SHPTP2 couples platelet-derived growth factor receptor beta to Ras. *Proc Natl Acad Sci U S A* 91:7335–7339. <https://doi.org/10.1073/pnas.91.15.7335>.
  27. Paruchuri V, Prasad A, McHugh K, Bhat HK, Polyak K, Ganju RK. 2008. S100A7-downregulation inhibits epidermal growth factor-induced signaling in breast cancer cells and blocks osteoclast formation. *PLoS One* 3:e1741. <https://doi.org/10.1371/journal.pone.0001741>.
  28. Miura K, Wakayama Y, Tanino M, Orba Y, Sawa H, Hatakeyama M, Tanaka S, Sabe H, Mochizuki N. 2013. Involvement of EphA2-mediated tyrosine phosphorylation of Shp2 in Shp2-regulated activation of extracellular signal-regulated kinase. *Oncogene* 32:5292–5301. <https://doi.org/10.1038/onc.2012.571>.
  29. Schaper F, Gendo C, Eck M, Schmitz J, Grimm C, Anhuif D, Kerr IM, Heinrich PC. 1998. Activation of the protein tyrosine phosphatase SHP2 via the interleukin-6 signal transducing receptor protein gp130 requires tyrosine kinase Jak1 and limits acute-phase protein expression. *Biochem J* 335:557–565. <https://doi.org/10.1042/bj3350557>.
  30. Ostman A, Hellberg C, Bohmer FD. 2006. Protein-tyrosine phosphatases and cancer. *Nat Rev Cancer* 6:307–320. <https://doi.org/10.1038/nrc1837>.
  31. Saxton TM, Ciruna BG, Holmyard D, Kulkarni S, Harpal K, Rossant J, Pawson T. 2000. The SH2 tyrosine phosphatase shp2 is required for mammalian limb development. *Nat Genet* 24:420–423. <https://doi.org/10.1038/74279>.
  32. Chernock RD, Cherla RP, Ganju RK. 2001. SHP2 and cbl participate in alpha-chemokine receptor CXCR4-mediated signaling pathways. *Blood* 97:608–615. <https://doi.org/10.1182/blood.v97.3.608>.
  33. Nakamura T, Gulick J, Colbert MC, Robbins J. 2009. Protein tyrosine phosphatase activity in the neural crest is essential for normal heart and skull development. *Proc Natl Acad Sci U S A* 106:11270–11275. <https://doi.org/10.1073/pnas.0902230106>.
  34. Yamamoto S, Yoshino I, Shimazaki T, Murohashi M, Hevner RF, Lax I, Okano H, Shibuya M, Schlessinger J, Gotoh N. 2005. Essential role of Shp2-binding sites on FRS2alpha for corticogenesis and for FGFR2-dependent proliferation of neural progenitor cells. *Proc Natl Acad Sci U S A* 102:15983–15988. <https://doi.org/10.1073/pnas.0507961102>.
  35. Tartaglia M, Mehler EL, Goldberg R, Zampino G, Brunner HG, Kremer H, van der Burgt I, Crosby AH, Ion A, Jeffery S, Kalidas K, Patton MA, Kucherlapati RS, Gelb BD. 2001. Mutations in PTPN11, encoding the protein tyrosine phosphatase SHP-2, cause Noonan syndrome. *Nat Genet* 29:465–468. <https://doi.org/10.1038/ng772>.
  36. Xu R, Yu Y, Zheng S, Zhao X, Dong Q, He Z, Liang Y, Lu Q, Fang Y, Gan X, Xu X, Zhang S, Dong Q, Zhang X, Feng G-S. 2005. Overexpression of Shp2 tyrosine phosphatase is implicated in leukemogenesis in adult human leukemia. *Blood* 106:3142–3149. <https://doi.org/10.1182/blood-2004-10-4057>.
  37. Zhou XD, Agazie YM. 2008. Inhibition of SHP2 leads to mesenchymal to epithelial transition in breast cancer cells. *Cell Death Differ* 15:988–996. <https://doi.org/10.1038/cdd.2008.54>.
  38. Lazzara MJ, Lane K, Chan R, Jasper PJ, Yaffe MB, Sorger PK, Jacks T, Neel BG, Lauffenburger DA. 2010. Impaired SHP2-mediated extracellular signal-regulated kinase activation contributes to gefitinib sensitivity of lung cancer cells with epidermal growth factor receptor-activating mutations. *Cancer Res* 70:3843–3850. <https://doi.org/10.1158/0008-5472.CAN-09-3421>.
  39. Conti E, Dottorini T, Sarkozy A, Tiller GE, Esposito G, Pizzuti A, Dallapiccola B. 2003. A novel PTPN11 mutation in LEOPARD syndrome. *Hum Mutat* 21:654. <https://doi.org/10.1002/humu.9149>.
  40. Wang JP, Bowen GN, Padden C, Cerny A, Finberg RW, Newburger PE, Kurt-Jones EA. 2008. Toll-like receptor-mediated activation of neutrophils by influenza A virus. *Blood* 112:2028–2034. <https://doi.org/10.1182/blood-2008-01-132860>.
  41. Bender A, Bui LK, Feldman MA, Larsson M, Bhardwaj N. 1995. Inactivated influenza virus, when presented on dendritic cells, elicits human CD8+ cytolytic T cell responses. *J Exp Med* 182:1663–1671. <https://doi.org/10.1084/jem.182.6.1663>.
  42. Kalinowski A, Galen BT, Ueki IF, Sun Y, Mullen A, Osafo-Addo A, Clark B, Joerns J, Liu W, Nadel JA, Dela Cruz CS, Koff JL. 2018. Respiratory syncytial virus activates epidermal growth factor receptor to suppress interferon regulatory factor 1-dependent interferon-lambda and antiviral defense in airway epithelium. *Mucosal Immunol* 11:958–967. <https://doi.org/10.1038/mi.2017.120>.
  43. Lupberger J, Duong FH, Fofana I, Zona L, Xiao F, Thumann C, Durand SC, Pessaux P, Zeisel MB, Heim MH, Baumert TF. 2013. Epidermal growth factor receptor signaling impairs the antiviral activity of interferon-alpha. *Hepatology* 58:1225–1235. <https://doi.org/10.1002/hep.26404>.
  44. Yang L, Xu J, Guo L, Guo T, Zhang L, Feng L, Chen H, Wang Y. 2018. Porcine epidemic diarrhea virus-induced epidermal growth factor receptor activation impairs the antiviral activity of type I interferon. *J Virol* 92:e02095-17. <https://doi.org/10.1128/JVI.02095-17>.
  45. Dai K, Huang L, Chen J, Yang L, Gong Z. 2015. Amphiregulin promotes the

- immunosuppressive activity of intrahepatic CD4(+) regulatory T cells to impair CD8(+) T-cell immunity against hepatitis B virus infection. *Immunology* 144:506–517. <https://doi.org/10.1111/imm.12400>.
46. Oshiumi H, Miyashita M, Okamoto M, Morioka Y, Okabe M, Matsumoto M, Seya T. 2015. DDX60 is involved in RIG-I-dependent and independent antiviral responses, and its function is attenuated by virus-induced EGFR activation. *Cell Rep* 11:1193–1207. <https://doi.org/10.1016/j.celrep.2015.04.047>.
  47. Chen Y-NP, LaMarche MJ, Chan HM, Fekkes P, Garcia-Fortanet J, Acker MG, Antonakos B, Chen CH-T, Chen Z, Cooke VG, Dobson JR, Deng Z, Fei F, Firestone B, Fodor M, Fridrich C, Gao H, Grunenfelder D, Hao H-X, Jacob J, Ho S, Hsiao K, Kang ZB, Karki R, Kato M, Larrow J, La Bonte LR, Lenoir F, Liu G, Liu S, Majumdar D, Meyer MJ, Palermo M, Perez L, Pu M, Price E, Quinn C, Shakya S, Shultz MD, Slisz J, Venkatesan K, Wang P, Warmuth M, Williams S, Yang G, Yuan J, Zhang J-H, Zhu P, Ramsey T, Keen NJ, et al. 2016. Allosteric inhibition of SHP2 phosphatase inhibits cancers driven by receptor tyrosine kinases. *Nature* 535:148–152. <https://doi.org/10.1038/nature18621>.
  48. Oishi K, Gaengel K, Krishnamoorthy S, Kamiya K, Kim IK, Ying H, Weber U, Perkins LA, Tartaglia M, Mlodzik M, Pick L, Gelb BD. 2006. Transgenic Drosophila models of Noonan syndrome causing PTPN11 gain-of-function mutations. *Hum Mol Genet* 15:543–553. <https://doi.org/10.1093/hmg/ddi471>.
  49. Mohi MG, Williams IR, Dearolf CR, Chan G, Kutok JL, Cohen S, Morgan K, Boulton C, Shigematsu H, Keilhack H, Akashi K, Gilliland DG, Neel BG. 2005. Prognostic, therapeutic, and mechanistic implications of a mouse model of leukemia evoked by Shp2 (PTPN11) mutations. *Cancer Cell* 7:179–191. <https://doi.org/10.1016/j.ccr.2005.01.010>.
  50. Chen YJ, Chien PH, Chen WS, Chien YF, Hsu YY, Wang LY, Chen JY, Lin CW, Huang TC, Yu YL, Huang WC. 2013. Hepatitis B virus-encoded X protein downregulates EGFR expression via inducing microRNA-7 in hepatocellular carcinoma cells. *Evid Based Complement Alternat Med* 2013:682380. <https://doi.org/10.1155/2013/682380>.
  51. Menzo S, Clementi M, Alfani E, Bagnarelli P, Iacovacci S, Manzin A, Dandri M, Natoli G, Levrero M, Carloni G. 1993. Trans-activation of epidermal growth factor receptor gene by the hepatitis B virus X-gene product. *Virology* 196:878–882. <https://doi.org/10.1006/viro.1993.1550>.
  52. Sheen TS, Huang YT, Chang YL, Ko JY, Wu CS, Yu YC, Tsai CH, Hsu MM. 1999. Epstein-Barr virus-encoded latent membrane protein 1 co-expresses with epidermal growth factor receptor in nasopharyngeal carcinoma. *Jpn J Cancer Res* 90:1285–1292. <https://doi.org/10.1111/j.1349-7006.1999.tb00710.x>.
  53. Badawy AA, El-Hindawi A, Hammam O, Moussa M, Gabal S, Said N. 2015. Impact of epidermal growth factor receptor and transforming growth factor-alpha on hepatitis C virus-induced hepatocarcinogenesis. *APMIS* 123:823–831. <https://doi.org/10.1111/apm.12431>.
  54. Venkataraman T, Coleman CM, Frieman MB. 2017. Overactive epidermal growth factor receptor signaling leads to increased fibrosis after severe acute respiratory syndrome coronavirus infection. *J Virol* 91:e00182-17. <https://doi.org/10.1128/JVI.00182-17>.
  55. Normanno N, De Luca A, Bianco C, Strizzi L, Mancino M, Maiello MR, Carotenuto A, De Feo G, Caponigro F, Salomon DS. 2006. Epidermal growth factor receptor (EGFR) signaling in cancer. *Gene* 366:2–16. <https://doi.org/10.1016/j.gene.2005.10.018>.
  56. Balasubramanian A, Ganju RK, Groopman JE. 2003. Hepatitis C virus and HIV envelope proteins collaboratively mediate interleukin-8 secretion through activation of p38 MAP kinase and SHP2 in hepatocytes. *J Biol Chem* 278:35755–35766. <https://doi.org/10.1074/jbc.M302889200>.
  57. Baron M, Davignon JL. 2008. Inhibition of IFN-gamma-induced STAT1 tyrosine phosphorylation by human CMV is mediated by SHP2. *J Immunol* 181:5530–5536. <https://doi.org/10.4049/jimmunol.181.8.5530>.
  58. Bakken T, He M, Cannon ML. 2010. The phosphatase Shp2 is required for signaling by the Kaposi's sarcoma-associated herpesvirus viral GPCR in primary endothelial cells. *Virology* 397:379–388. <https://doi.org/10.1016/j.virol.2009.11.030>.
  59. Philpott N, Bakken T, Pennell C, Chen L, Wu J, Cannon M. 2011. The Kaposi's sarcoma-associated herpesvirus G protein-coupled receptor contains an immunoreceptor tyrosine-based inhibitory motif that activates Shp2. *J Virol* 85:1140–1144. <https://doi.org/10.1128/JVI.01362-10>.
  60. Bixler SL, Sandler NG, Douek DC, Mattapallil JJ. 2013. Suppressed Th17 levels correlate with elevated PIAS3, SHP2, and SOCS3 expression in CD4 T cells during acute simian immunodeficiency virus infection. *J Virol* 87:7093–7101. <https://doi.org/10.1128/JVI.00600-13>.
  61. Ouyang W, Liu C, Pan Y, Han Y, Yang L, Xia J, Xu F. 2020. SHP2 deficiency promotes *Staphylococcus aureus* pneumonia following influenza infection. *Cell Prolif* 53:e12721. <https://doi.org/10.1111/cpr.12721>.
  62. Araki T, Nawa H, Neel BG. 2003. Tyrosyl phosphorylation of Shp2 is required for normal ERK activation in response to some, but not all, growth factors. *J Biol Chem* 278:41677–41684. <https://doi.org/10.1074/jbc.M306461200>.
  63. Agazie YM, Movilla N, Ischenko I, Hayman MJ. 2003. The phosphotyrosine phosphatase SHP2 is a critical mediator of transformation induced by the oncogenic fibroblast growth factor receptor 3. *Oncogene* 22:6909–6918. <https://doi.org/10.1038/sj.onc.1206798>.
  64. Kang HJ, Chung DH, Sung CO, Yoo SH, Yu E, Kim N, Lee SH, Song JY, Kim CJ, Choi J. 2017. SHP2 is induced by the HBx-NF-kappaB pathway and contributes to fibrosis during human early hepatocellular carcinoma development. *Oncotarget* 8:27263–27276. <https://doi.org/10.18632/oncotarget.15930>.
  65. Wang ZF, Liu XL, Zhao ZD, Xu CF, Zhang K, Chen CW, Sun L, Gao GF, Ye X, Liu WJ. 2011. Cyclophilin E functions as a negative regulator to influenza virus replication by impairing the formation of the viral ribonucleoprotein complex. *PLoS One* 6:e22625. <https://doi.org/10.1371/journal.pone.0022625>.
  66. Fan KW, Jia YP, Wang S, Li H, Wu DF, Wang GS, Chen JL. 2012. Role of Itk signalling in the interaction between influenza A virus and T-cells. *J Gen Virol* 93:987–997. <https://doi.org/10.1099/vir.0.041228-0>.
  67. Pan Q, Zhao Z, Liao Y, Chiu SH, Wang S, Chen B, Chen N, Chen Y, Chen JL. 2019. Identification of an interferon-stimulated long noncoding RNA (LncRNA ISR) involved in regulation of influenza A virus replication. *Int J Mol Sci* 20:5118. <https://doi.org/10.3390/ijms20205118>.